Neutrino-nuclear response and photonuclear reactions

H. Ejiri*
Research Center for Nuclear Physics, Osaka University, Ibaraki, Osaka 567-0047, Japan and Nuclear Science, Czech Technical University, Prague, Czech Republic

A. I. Titov
Joint Institute of Nuclear Research, 141980 Dubna, Russia

M. Boswell
Los Alamos National Laboratory, Los Alamos, New Mexico, USA

A. Young
Department of Physics, North Carolina State University, Raleigh, North Carolina, USA
(Received 26 March 2013; revised manuscript received 23 October 2013; published 18 November 2013)

Photonuclear reactions are shown to be used for studying neutrino (weak) nuclear responses involved in astroneutrino nuclear interactions and double beta decays. Charged current weak responses for ground and excited states are studied by using photonuclear reactions through isobaric analog states of those states, while neutral current weak responses for excited states are studied by using photonuclear reactions through the excited states. The weak interaction strengths are studied by measuring the cross sections of the photonuclear reactions, and the spin and parity of the states are studied by measuring angular correlations of particles emitted from the photonuclear reactions. Medium-energy polarized photons obtained from laser photons scattered off GeV electrons are very useful. Nuclear responses studied by photonuclear reactions are used to evaluate neutrino (weak) nuclear responses, i.e., nuclear beta and double beta matrix elements and neutrino-nuclear interactions, and to verify theoretical calculations for them.

DOI: 10.1103/PhysRevC.88.054610 PACS number(s): 25.20.−x, 23.20.−g, 23.40.−s, 24.70.+s

I. INTRODUCTION

Fundamental properties of neutrinos and astroneutrino nuclear interactions are studied by investigating nuclear double beta ($\beta\beta$) decays, nuclear inverse beta (β) decays, and neutral current nuclear excitations. Here nuclear weak responses (the square of the nuclear matrix element) are crucial to studying neutrino properties of particle and astrophysical interest [1–3].

Neutrinoless double beta decays ($0\nu\beta\beta$) are the most sensitive and realistic probes to study the Majorana properties of neutrinos: their absolute mass scales and mass spectrum, the lepton-sector CP phases, and other properties beyond the standard model. They are discussed in review papers and references therein [2–7]. The $0\nu\beta\beta$ transition rate via the ν-mass process is given in terms of the effective ν mass m_ν as

$$T^{0\nu} = G^{0\nu}(M^{0\nu})^2(m_\nu)^2, \tag{1}$$

where $T^{0\nu}$ is the transition rate, $G^{0\nu}$ is the phase space factor, and $M^{0\nu}$ is the $0\nu\beta\beta$ matrix element. Thus one needs the $0\nu\beta\beta$ matrix element $M^{0\nu}$ to design the optimum detector and to extract the neutrino mass from $0\nu\beta\beta$ rate when it is observed.

The $0\nu\beta\beta$ matrix element is expressed as $M^{0\nu} = \sum_k M_k^{\beta\beta}$, where $M_k^{\beta\beta}$ are the $0\nu\beta\beta$ matrix elements via the kth state in the intermediate nucleus. Then the single β matrix elements of $M_k(\beta^-)$ and $M_k(\beta^+)$ for the β transitions via the kth intermediate state can be used to help evaluate the $\beta\beta$ matrix element of $M_k^{\beta\beta}$ involved in $M^{0\nu}$. The $0\nu\beta\beta$ decay is associated with medium momentum exchange of an intermediate virtual neutrino, and accordingly the intermediate states involved are the ground and excited states with angular momenta of $l \approx 1$–3.

Astroneutrino charged current (CC) interactions are studied by measuring the inverse $\beta^\pm$ decays induced by the neutrinos, and then the β matrix elements of $M(\beta^\pm)$ are needed to study the interactions. Similarly neutral current (NC) studies require the NC matrix element.

Accurate calculations of β and $\beta\beta$ matrix elements are hard since they are sensitive to nuclear spin-isospin correlations, nuclear medium effects, and nuclear structures, as discussed in the review articles [1,2,7–9]. Accordingly, experimental studies of them are of great interest [1–3,5,7].

The nuclear weak responses (matrix elements) are studied experimentally by using neutrino or muon probes with weak interactions, photon probes with electromagnetic (EM) interactions, and nuclear probes with strong nuclear interactions [1,3,6,7], as shown in Fig. 1.

Neutrino beams could be useful if intense neutrino beams and multiton-scale detectors might be available. The neutrinos from the Spallation Neutron Source (SNS) and the Japan Proton Accelerator Research Complex (J-PARC) are of great interest [2,10,11]. Recently μ capture reactions are shown to be used to study β^+ strengths [3,12,13].

Charge exchange reactions by using nuclear probes have been extensively used for evaluating CC $\beta^\pm$ responses. The high energy-resolution (^{3}He,t) reaction at the Research Center for Nuclear Physics (RCNP, Osaka) is very powerful for

*ejiri@rcnp.osaka-u.ac.jp

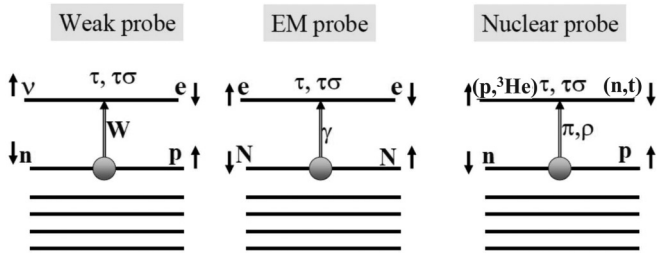

FIG. 1. Nuclear spin (σ) and isospin (τ) responses for CC weak interactions and their studies by neutrino (ν) probes via weak interaction, γ probes via EM interaction, and by nuclear probes via strong nuclear interaction [1,2].

studying CC β^- responses [7,14–16]. CC β^+ response studies by (t,^{3}He) reactions require radioactive t beams [17], and those by (d,^{2}He) reactions need a big spectrometer for $^2\mathrm{He} \to 2p$ [18].

The present work aims at reporting possible photonuclear reactions by using high quality EM photon probes for CC β^+ and NC responses. In fact, weak and EM responses have similar spin-isospin operators, and thus the EM responses are used to evaluate the weak ones, and vice versa, as used for transitions via the isobaric analog state (IAS) [19–21] and also for electron scattering and other application [22–24]. The use of EM probes for $\beta\beta$ response studies is discussed in reviews [6,10]. Unique features of EM photon probes are as follows.

(i) EM interactions involved in photonuclear reactions are well known. The dominant lowest multipole transition is well evaluated within the long-wave-length approximation in the present excitation region.
(ii) NC and CC β^+ responses for nuclear ground and excited states are studied by measuring photo-nuclear excitations of them and those of the IASs, respectively.
(iii) Vector (τ isospin) and axial vector ($\sigma\tau$ spin isospin) responses are studied by measuring electric (E) and magnetic (M) photonuclear excitations, respectively.
(iv) Spin and parity of the state are determined by measuring angular correlations of photonuclear reactions with polarized photons.
(v) EM interactions are simple and photon probes are not distorted in nuclei, while nuclear interactions involved in nuclear probes are rather complicated and nuclear beams are distorted by nuclear potential.
(vi) High energy-resolution intense photon beams with large polarization are obtained from polarized laser photons scattered off GeV electrons.

II. WEAK RESPONSES STUDIED BY PHOTO NUCLEAR REACTIONS

Weak and EM transitions to be discussed in the present paper are the vector and EL ($E1$, $E2$) transitions with natural parity $J^P = 1^-, 2^+$ and the axial-vector and ML ($M1$, $M2$) transitions with unnatural parity $J^\pi = 1^+, 2^-$. The weak vector and axial-vector transition operators are expressed as [1,22,24]

$$T(VL) = g_V \tau^i r^L Y_L, \quad L = 1, 2, \tag{2}$$

$$T(AVL) = g_A \tau^i [\sigma \times r^{L-1} Y_{L-1}]_L, \quad L = 1, 2, \tag{3}$$

where g_V and g_A are the vector and axial-vector weak coupling constants, and τ^3 and $\tau^\pm$ are NC and CC isospin operators. The EM transition operators corresponding to the VL and AVL weak ones are expressed as [1,22,24]

$$T(EL) = g_{EL} r^L Y_L, \tag{4}$$

$$T(ML) = g_S [\sigma \times r^{L-1} Y_{L-1}]_L + g_L [j \times r^{L-1} Y_{L-1}]_L, \tag{5}$$

$$g_S = \frac{e\hbar}{2Mc} [L(2L+1)]^{1/2} \left[\frac{g_s}{2} - \frac{g_l}{L+1} \right], \tag{6}$$

$$g_L = \frac{2 g_l}{L+1}, \tag{7}$$

where g_{EL}, g_s, and g_l are the EM coupling constant (effective charge), the spin g factor, and the orbital g factor, respectively. In case of spin stretched ML transitions of $J \to J \pm L$, the second term of $T(ML)$ vanishes, and the transition operator is given by the first term of Eq. (5) [22,24]. Then experimental studies of EL and ML transition rates are used to evaluate the analogous vector and axial-vector weak responses.

The weak axial-vector transitions of $T(AVJ) = g_A \tau^i [\sigma \times r Y_1]_J$ with $J^\pi = 0^-, 1^-, 2^-$ are of the same order of magnitude as $T(V1)$. However, the corresponding EM transitions are 2–3 orders of magnitude weaker than $T(E1)$. Then the 1^- contribution is negligible compared with the $E1$ transition. There is no $0^+ \to 0^- \gamma$ transition. Thus we discuss only $J^\pi = 2^-$.

The EM coupling constant depends on the isospin z component, namely on the proton or neutron. Using the isospin operator τ^3 and $\tau^0 = 1$, the coupling constant is expressed as

$$g_i = \frac{g_i(V)}{2} \tau^3 + \frac{g_i(S)}{2} \tau^0, \tag{8}$$

where g_i with $i = E, s$, and l are the electric, the magnetic spin, and the magnetic orbital coupling constants, and $g_i(V)$ and $g_i(S)$ are the corresponding isovector and isoscalar coupling constants. They are written by using the neutron and proton coupling constants as $g_i(V) = g_i(n) - g_i(p)$ and $g_i(S) = g_i(n) + g_i(p)$.

The EM transition matrix element includes both the isovector and isoscalar components, and they are modified differently by nuclear spin-isospin correlations and nuclear medium effects. Consequently, the isovector weak matrix element is not exactly the same as the corresponding EM matrix element. Nevertheless, the measured EM matrix element helps evaluate the weak matrix element and check or confirm theoretical calculations of the weak matrix element. The IAS provides a unique opportunity to select exclusively the isovector component of the EM transition, which is analogous to the β^+ transition. So, we discusses mainly IAS γ transitions in the present paper.

III. PHOTONUCLEAR REACTIONS VIA ISOBARIC STATES

CC β^+ responses are studied by photo nuclear reactions through the IAS, as shown by the γ decays from the IAS

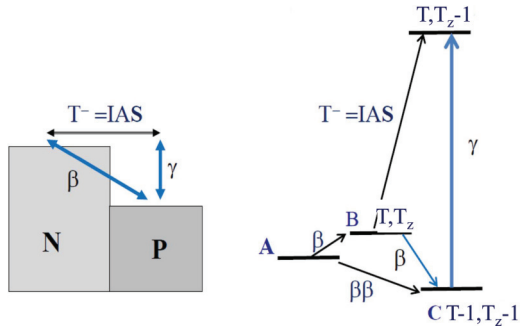

FIG. 2. (Color online) Level and transition schemes of single β and double β transitions and γ transitions via IAS. T^- is the isospin lowering operator to transfer a state to IAS [19–21]. T_z $(=T)$ is the isospin z component.

[19–21]. The β and γ matrix elements are related as

$$\langle f|gm^{\beta}|i\rangle \approx \frac{g}{e}K\langle f|em^{\gamma}|\mathrm{IAS}\rangle, \tag{9}$$

where gm^{β} and em^{γ} are analogous β and γ transition operators with g and e being the weak and EM coupling constants, $K = (2T)^{1/2}$ is the normalization constant, and $|\mathrm{IAS}\rangle = K^{-1}T^-|i\rangle$ with T^- being the isospin lowering operator.

The relation between the weak and EM matrix elements for IAS transitions is based on the rotation (T^-) symmetry in the isospin space. Then one can obtain the β matrix element for $|f\rangle \rightarrow |i\rangle$ by observing the analogous γ absorption for $|f\rangle \rightarrow |\mathrm{IAS}\rangle$. Here $|f\rangle$ and $|i\rangle$ are the final and intermediate states in the $\beta\beta$ decay, and the initial and final nuclei in the antineutrino CC nuclear interaction. This is a useful method used extensively for (p,γ) reactions through the IAS on various nuclei as discussed in [25]. The β, $\beta\beta$, and analogous γ transitions are schematically shown in Fig. 2.

In medium and heavy nuclei, the IAS is observed as an isobaric analog resonance (IAR) in the medium-excitation region. The photonuclear cross section via the IAR with J^{π} is expressed as

$$\sigma(\gamma,n) = \frac{S(2J+1)\pi}{k_{\gamma}^2}\frac{\Gamma_{\gamma}\Gamma_n}{(E-E_R)^2+\Gamma_t^2/4}, \tag{10}$$

where Γ_{γ}, Γ_t, and Γ_n are the γ capture width, the total width, and the neutron decay width, S is the spin factor, and k_{γ} is the incident photon momentum.

The integrated photonuclear cross section is given by

$$\int \sigma(\gamma,n)dE = \frac{S(2J+1)2\pi^2}{k_{\gamma}^2}\frac{\Gamma_{\gamma}\Gamma_n}{\Gamma_t}. \tag{11}$$

.

IAR at the excitation region well above the particle threshold energy decays by emitting mostly neutrons since proton decays are suppressed by the Coulomb barrier. Then one gets $\Gamma_t \approx \Gamma_n$, where Γ_n is the sum of the neutron decay widths to all states. In the case of the $0^+ \rightarrow 1^{\pm}$ excitation in even-even nuclei, the Γ_{γ} width is obtained from the measured integrated cross section $\int \sigma(\gamma,n)dE = \pi^2 k_{\gamma}^{-2}\Gamma_{\gamma}$, where $\sigma(\gamma,n)$ is the sum of the (γ,n) cross sections for neutron decays to all final states.

Now we discuss photonuclear cross sections for $E1$ and $M1$ photoexcitations on even-even nuclei with $J^{\pi} = 0^+$. The reduced widths of $\Gamma_{\gamma}(E1)$ and $\Gamma_{\gamma}(M1)$ are expressed, respectively, in terms of the $E1$ and $M1$ matrix elements of $M(E1)efm$ and $M(M1)e\hbar/(2Mc)$ and in terms the excitation (photon) energy E_{γ} in units of MeV as [22]

$$\Gamma_{\gamma}(E1) = 1.59\times 10^{15}E^3M(E1)^2/\mathrm{s}, \tag{12}$$

$$\Gamma_{\gamma}(M1) = 1.76\times 10^{13}E^3M(M1)^2/\mathrm{s}. \tag{13}$$

The $M(E1)$ and $M(M1)$ for IAR are expressed as $M(E1) = M_1(E1)/K$ and $M(M1) = M_1(M1)/K$, where $M_1(E1)$ and $M_1(M1)$ are the corresponding isovestor γ matrix elements.

The matrix elements for typical $E1$ and $M1$ excitations on medium-heavy nuclei in the mass region of $A = 100$, $T = 8$, $K = 4$ are $M_1(E1) \approx 0.125$ [24] and $M_1(M1) \approx 1.15$ [24]. Using these values, for example, one gets $M(E1) \approx 0.03$ and $M(M1) \approx 0.28$ for the photon absorption into the IAS. The IAR excitation energy is around $E = 8$ MeV in this mass region. Then the cross sections are obtained as

$$\int \sigma(\gamma,n)dE = 2.9\times 10^{-3}\ \mathrm{MeV\,fm^2} \quad (E1), \tag{14}$$

$$\int \sigma(\gamma,n)dE = 2.7\times 10^{-3}\ \mathrm{MeV\,fm^2} \quad (M1). \tag{15}$$

Then the counting rates with a typical target of 10 g/cm^2 are $Y(E1) = 1.7\times 10^{-6}\epsilon N_{\gamma}/\mathrm{s}$ and $Y(M1) = 1.6\times 10^{-6}\epsilon N_{\gamma}/\mathrm{s}$, where N_{γ} is the number of photons per second per MeV and ϵ is the detection efficiency. Thus experimental studies of these photo nuclear reactions are quite realistic by using medium energy photons with $N_{\gamma} \approx 10^{8-9}/(\mathrm{MeV\ s})$.

In heavy nuclei, IAR shows up as a sharp resonance on the top of the $E1$ giant resonance (GR). Then the $E1$ photonuclear reaction is given by [21]

$$\frac{d\sigma(\gamma,n)}{d\Omega} = k\left[A_I^2 + A_G^2 + 2\,\mathrm{Re}(A_I A_G e^{i\phi})\right], \tag{16}$$

where A_I and A_G are the IAR and GR amplitudes and the third term is the interference term with ϕ being the relative phase. It is noted that the phase of the matrix element can be determined from the interference pattern.

The two-neutrino $\beta\beta$ matrix element is expressed by the sum of the products of the single β^- and β^+ matrix elements via low-lying intermediate 1^+ states [5]. Similarly, the $0\nu\beta\beta$ matrix element may be given approximately by those of the single β^- and β^+ matrix elements via low-lying intermediate states with $J^{\pi} = 0^{\pm}$, $1^{\pm}$, $2^{\pm}$, $3^{\pm}$ and so on. In cases of medium energy neutrino interactions, $0^{\pm}$, $1^{\pm}$, $2^{\pm}$ states are involved. The single β^+ matrix elements for the $1^{\pm}$ states are studied by measuring photonuclear reactions via the IASs of the $1^{\pm}$ states.

IV. ANGULAR CORRELATIONS OF PHOTONUCLEAR REACTIONS

Nuclear states excited by medium-energy photons decay by emitting mostly neutrons. The spin and parity of the excited state are identified by measuring angular distributions of the

emitted particles with respect to the photon beam and its polarization.

Let us consider the photonuclear reaction on an even-even nucleus by using linearly polarized photons $\vec{\gamma}$,

$$\vec{\gamma} + N(0^+) \to N^*(J^P) \to N_r\left(J_r^P\right) + n, \tag{17}$$

where N, N^*, and N_r are the target nucleus in the ground state, the excited nucleus, and the outgoing recoil nucleus, respectively, with corresponding spin-parities of 0^+, J^P, and J_r^P, and n is the outgoing neutron. We calculate the azimuthal and polar angular distributions of the outgoing neutron. We choose the z axis along the incoming photon momentum, and the x axis along the photon polarization.

The angular distribution is defined as

$$W(\theta, \phi) = \sum_{\sigma M_r} |A^S(J J_r \sigma M_r \theta\phi)|^2, \tag{18}$$

where A^S is the amplitude for excitation of the target nucleus to the excited state and subsequent decay to the recoil nucleus and the neutron. The superscript S stands for natural ($S = \mathrm{N}$) or unnatural ($S = \mathrm{U}$) spin-parity excitation. M_r and σ are the spin projections of the recoil nucleus and the neutron, respectively, and θ and ϕ are the polar and the azimuthal angles of the neutron momentum, respectively. The angular distribution is normalized as

$$\int W(\theta, \phi)\, d\cos\theta\, d\phi = 1. \tag{19}$$

The transition amplitude is given as

$$A^S(J J_r \sigma M_r \theta\phi) = \sum_{lm} a_l C^S(J J_r l m \sigma M_r) Y_{lm}(\theta\phi), \tag{20}$$

where a_l is the partial amplitude of the neutron decay with orbital angular momentum l, and C^S is the coefficient for the angular momentum couplings as written in terms of the Clebsch-Gordan coefficients for the coupling of the angular momenta involved in the reaction.

Let us consider photonuclear reactions on two typical nuclei of ^{76}Se and ^{100}Mo [26]. The photo excitations discussed are the EM transitions to the IASs of ^{76}As and ^{100}Tc. Thus they are used to evaluate the analogous weak transitions to ^{76}As and ^{100}Tc with the same multipole and spin-parity:

$$\vec{\gamma} + {}^{76}\mathrm{Se} \to {}^{76}\mathrm{Se}(J^p) \to {}^{75}\mathrm{Se}\left(\tfrac{3}{2}^-\right) + n, \tag{21}$$

$$\vec{\gamma} + {}^{100}\mathrm{Mo} \to {}^{100}\mathrm{Mo}(J^p) \to {}^{99}\mathrm{Mo}\left(\tfrac{1}{2}^+\right) + n. \tag{22}$$

The odd neutron of the recoil nucleus ^{75}Se is in the orbital p state, while that of the recoil nucleus ^{99}Mo is in the s state. This difference is important for the angular distribution of the outgoing neutron. We will consider the azimuthal angular distribution at the fixed polar angle $\theta = \pi/2$ and the polar angular distribution at the fixed azimuthal angle $\phi = \pi/2$.

A. Natural parity excitations

The angular distributions for natural parity 1^- excitations are presented in Fig. 3. In case of Se, the possible orbital configurations of the outgoing neutron from the 1^- state to the $(3/2)^-$ ground state in ^{75}Se are s ($l = 0$) and d ($l = 2$). The first

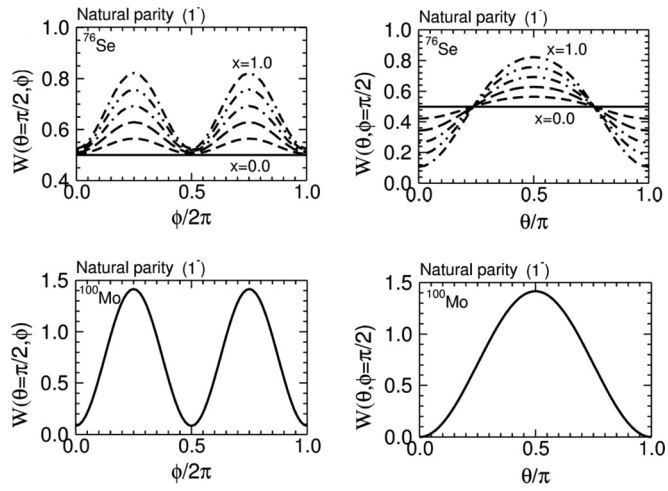

FIG. 3. Top: Azimuthal (left) and polar (right) angular distributions (relative) of the neutron from the 1^- photonuclear excitation on ^{76}Se with x being the fraction of the d configuration (see text). Bottom: The angular distributions for ^{100}Mo.

case leads to the isotropic distribution, while the second one gives the anisotropic distribution, determined by Y_2-spherical harmonics. We introduce a variable x defined as the relative probability of d neutron emission. It is proportional to $a_{l=2}^2$. We use x as a parameter that varies from 0 to 1.0. The distributions with $x = 0$, 0.2, 0.4, 0.6, 0.8, and 1.0 are shown in Fig. 3. In the case of Mo, only p ($l = 1$) neutron emission is allowed from the 1^- state to the $(1/2)^+$ ground state in ^{99}Mo. The distribution is close to (but not exactly) $\sin^2\phi$.

The angular distributions for natural parity 2^+ excitations are shown in Fig. 4. In the case of Se, the possible orbital configurations of the outgoing neutron to the $(3/2)^-$ ground state in ^{75}Se are p and f ($l = 3$). Here x is the relative probability of the f neutron. Then, the angular distribution is defined by Y_1 and Y_3 spherical harmonics. In the case of the Mo nucleus, only the d configuration is allowed, which results in superposition of Y_2^2 harmonics.

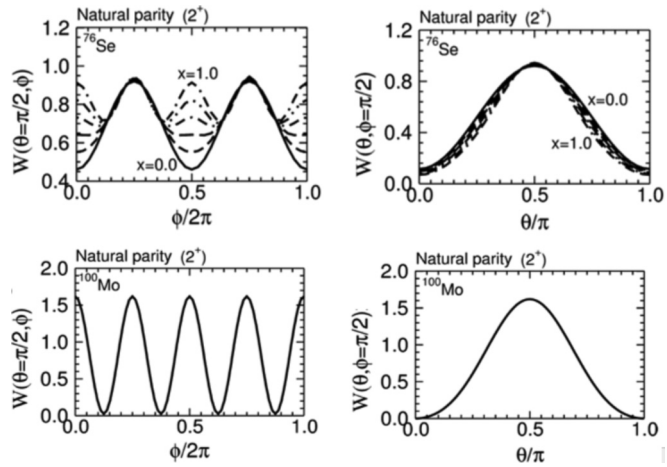

FIG. 4. Top: Azimuthal (left) and polar (right) angular distributions (relative) of the neutron from the 2^+ photonuclear excitation on ^{76}Se with x being the fraction of the f configuration (see text). Bottom: The angular distributions for ^{100}Mo.

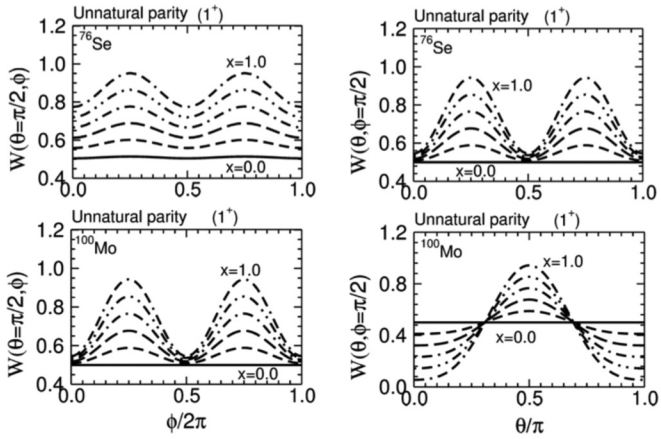

FIG. 5. Top: Azimuthal (left) and polar (right) angular distributions (relative) of the neutron from the 1^+ photonuclear excitation on ^{76}Se with x being the fraction of the f configuration (see text). Bottom: The angular distributions for ^{100}Mo with x being the fraction of the d configuration (see text).

B. Unnatural parity states

The angular distributions for unnatural parity 1^+ excitations are presented in Fig. 5. In the case of Se, the possible orbital configurations of the outgoing neutron to the $(3/2)^-$ ground state in ^{75}Se are p and f, which result in anisotropic ϕ dependence with maxima at $\phi = \pi/2$ and $3\pi/2$. In Fig. 5 the variable x denotes the relative contribution of the f orbital neutron. The distributions for $x = 0$ are not quite different from those for the natural parity 1^- state. Then, measurements of the neutron decays to other excited states also can be used to identify the spin-parity of the state. In the case of Mo, the s and d configurations contribute. Then one gets the anisotropic distribution by interplay of Y_0^2 and Y_2^2 harmonics, depending on the relative weight x of the d neutron.

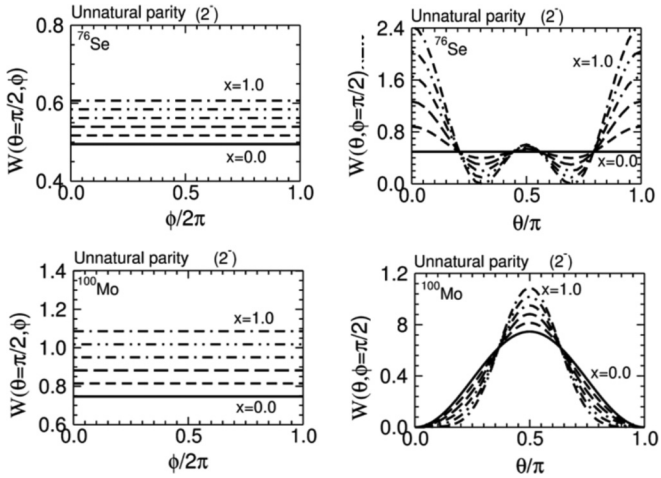

FIG. 6. Top: Azimuthal (left) and polar (right) angular distributions (relative) of the neutron from the 2^- photonuclear excitation on ^{76}Se with x being the fraction of the d configuration (see text). Bottom: The angular distributions for ^{100}Mo with x being the fraction of the f configuration (see text).

Angular distributions of neutrons from an unnatural parity 2^- state are shown in Fig. 6. In the case of Se, s and d orbital configurations are involved. Here x is the relative probability of the d neutron. The angular distributions are given by interplay of Y_0^2 and Y_2^2 for s and d, respectively. The first one gives an isotropic distribution. In the second case, the sum over the M_r and spin projections results in isotropic ϕ dependence. For the Mo nucleus, the p and f configurations give the angular distribution defined by an interplay of Y_1^2 and Y_3^2 harmonics. Here x is the relative probability of the f neutron. The sum over the neutron spin projection results in anisotropic ϕ dependence.

V. REMARKS

The present paper shows by theoretical considerations and calculations that NC and CC β^+ weak responses are studied by using photonuclear excitations. The EM coupling constant given in Eq. (5) is mainly the spin (g_s) component in the case of the isovector IAS transition as the axial-vector weak coupling constant. Then they are renormalized similarly by spin-isospin correlations. Thus the EM matrix element can be used to evaluate the single β^+ (weak) matrix element associated with the $0\nu\beta\beta$ matrix element. Actually, the renormalization effects on weak and EM transitions are in general not exactly the same, and one needs to carefully consider the possible state dependence in cases of EM transitions to different (non-IAS) states.

The β transition operator of the first forbidden β decays with $\Delta J = 1$ includes three terms of $T(rY1)$, $T(\alpha)$, and $T(\sigma \times rY_1)_1$. Then the term $T(rY1)$ is derived from the analogous $E1$ transition, and the term $T(\alpha)$ relative to $T(rY_1)$ is evaluated from the Conserved Vector Current (CVC) theory. Therefore, the spin matrix element $M(\sigma \times rY_1)_1$ can be deduced if both the β and γ transition rates are measured [20,21].

Experimental studies of $E1$ and $M1$ photonuclear reactions are quite realistic, while studies of $E2$ excitations require very intense photon beams. $M2$ excitations could hardly be realistic because of very small cross sections. Inelastic electron scatterings for them are interesting.

The High Intensity γ-ray Source (HIGS) is very attractive. The intense γ rays with $E = 2$–70 MeV, $\Delta E/E \approx 1\%$, and $I_\gamma \approx 10^7$/(MeV s) are obtained by intracavity Compton backscattering of Free Electron Laser (FEL) photons off 1.2 GeV electrons at the Duke Storage Ring [27]. Possible studies of photonuclear excitations of the IAS in ^{76}Se were discussed [28]. The photon intensity will be increased by two orders of magnitude in the future. Canadian Light Source (CLS) aims at intense photons from CO_2 lasers scattered off the 3 GeV electrons in the CLS ring [29]. The laser-backscattered source at NewSUBARU provides γ rays with $E =$ 17–40 MeV, $\Delta E/E = 2\%$ and $I_\gamma \approx 10^7$/s [30]. These photons are promising photon probes for the present photonuclear reactions.

ACKNOWLEDGMENTS

The authors thank Prof. W. Tornow, TUNL and Prof. H. Weller, TUNL for valuable discussions.

[1] H. Ejiri, Phys. Rep. C **338**, 265 (2000), and references therein.
[2] H. Ejiri, J. Phys. Soc. Jpn. **74**, 2101 (2005).
[3] H. Ejiri, Czechoslovak J. Phys. **56**, 459 (2006).
[4] F. Avignone, S. R. Elliott, and J. Engel, Rev. Mod. Phys. **80**, 481 (2008).
[5] H. Ejiri, J. Phys. Soc. Jpn. **78**, 074201 (2009).
[6] H. Ejiri, Prog. Part. Nucl. Phys. **64**, 249 (2010).
[7] J. Vergados, H. Ejiri, and F. Simkovic, Rep. Prog. Phys. **75**, 106301 (2012).
[8] J. Suhonen and O. Civitarese, Phys. Rep. **300**, 123 (1998).
[9] F. Simkovic, R. Hodak, A. Faessler, and P. Vogel, Phys. Rev. C **83**, 015502 (2011).
[10] H. Ejiri, Nucl. Instrum. Methods A **503**, 276 (2003).
[11] F. Avignone, in Workshop on Neutron and Nuclear Physics at the Stopped $\pi\mu$ Facility, Oak Ridge, 2000 (unpublished).
[12] J. Suhonen and M. Kortelainen, Czech J. Phys. **56**, 519 (2006).
[13] H. Ejiri *et al*., J. Phys. Soc. Jpn. **82**, 044202 (2013).
[14] H. Akimune *et al*., Phys. Lett. B **394**, 23 (1997).
[15] J. H. Thies *et al*., Phys. Rev. C **86**, 014304 (2012).
[16] J. H. Thies *et al*., Phys. Rev. C **86**, 044309 (2012).
[17] C. J. Guess *et al*., Phys. Rev. C **83**, 064318 (2011).
[18] H. Dohmann *et al*., Phys. Rev. C **78**, 041602(R) (2008).
[19] J.-I. Fujita, Phys. Lett. B **24**, 123 (1967).
[20] H. Ejiri *et al*., Phys. Rev. Lett. **21**, 373 (1968).
[21] H. Ejiri *et al*., Nucl. Phys. **128**, 388 (1969).
[22] A. Bohr and B. Mottelson, *Nuclear Structure II* (W. A. Benjamin, Reading, MA, 1975).
[23] T. W. Donnelly and J. D. Walecka, Annu. Rev. Nucl. Sci. **25**, 329 (1975).
[24] H. Ejiri and J. I. Fujita, Phys. Rep. C **38**, 86 (1978), and references therein.
[25] H. Ejiri and M. J. A. de Voigt, *Gamma Ray and Electron Spectroscopy in Nuclear Physics* (Oxford University Press, Oxford, 1989).
[26] National Nuclear Data Center, Brookhaven National Laboratory, http://www.nndc.bnl.gov
[27] H. R. Weller, H. W. Ahmed, H. Gao, W. Tornow, Y. K. Wu, M. Gai, and R. Miskimen, Prog. Part. Nucl. Phys. **62**, 257 (2009).
[28] M. Boswell, A. Young, and H. Ejiri, presented in NDM12 workshop on Neutrinos and Dark Matter in Nuclear Physics, Nara, Japan, June 2013.
[29] B. Szpunar, C. Rangacharyulu, S. Date, and H. Ejiri, Nucl. Instrum. Methods A **729**, 41 (2013).
[30] S. Miyamoto (private communication).